ELSEVIER

Materials Chemistry and Physics 40 (1995) 168–172

MATERIALS CHEMISTRY AND PHYSICS

The effects of Nd_2O_3 additives and Al_2O_3–SiO_2–TiO_2 sintering aids on the electrical resistivity of (Ba,Sr)TiO_3 PTCR ceramics

Chun-Hung Lai [a], Chen-Tsang Weng [b], Tseung-Yuen Tseng [b,*]

[a] *Department of Electronics Engineering, Lien-Ho College of Technology and Commerce, Miao-Li, Taiwan, ROC*

[b] *Department of Electronics Engineering and Institute of Electronics, National Chiao-Tung University, Hsinchu, Taiwan, ROC*

Received 28 January 1994; accepted 28 December 1994

Abstract

The influences of Nd donors and Al_2O_3–SiO_2–TiO_2 (AST) sintering aids on the electrical properties of (Ba,Sr)TiO_3 materials have been investigated. The room-temperature resistivity and the temperature coefficient of the anomalous resistivity rise were used to characterize the performance of the samples. From derivations based on the Heywang–Jonker barrier model, both characterizing parameters are expected to increase as a result of higher acceptor-state density at the grain boundary. The surface acceptor density, whose value was extracted from the slope in the Arrhenius plot of resistivity versus $1/(T\epsilon_m)$, where ϵ_m is the measured permittivity and T the absolute temperature, was found to decrease with the Nd content and increase with the AST dopant. A satisfactory interpretation of the observed variations in resistivity–temperature curves caused by additions of various dopants was thus obtained in the light of the resultant acceptor state density.

Keywords: Positive temperature coefficient of resistance; Acceptor-state density; Grain boundaries; Permittivity; Barriers

1. Introduction

Doped $BaTiO_3$ ceramic semiconductors exhibit the property of positive temperature coefficient of resistance (PTCR) [1]. The transition temperature, which is near the ferroelectric Curie point T_c, shifts to lower temperature upon substitution of Sr^{2+} for Ba^{2+}. Those PTC resistors with different 'switching' temperatures can find applications in current limiters and thermal controllers [2,3]. In view of these potentials, various fabrication techniques have been attempted to investigate the PTCR behavior and to improve the specimen performance. However, most of the reports are restricted to pure $BaTiO_3$ ceramics with a 120 °C Curie point [1,4–6].

The PTCR phenomenon is found only for ceramic materials. The presence of grain boundaries, in which the surface states reside and act as the trap centers for charge carriers, is therefore believed to be responsible for the PTCR effect. A widely accepted model that elucidates the conduction mechanism of the PTCR phenomenon has been proposed by Heywang and Jonker [4–6]. Heywang ascribed the anomalous rise in resistivity for $T > T_c$ to the formation of a Schottky barrier, whose height increases owing to the decreasing permittivity (Curie–Weiss behavior). Jonker then modified this model by considering the nonvanishing spontaneous polarization to explain the simultaneous low resistivity and low permittivity at $T < T_c$. In view of this anomalous resistivity jump, observed only in semiconducting ceramics, and being strongly influenced by the acceptor states in the scheme of the Heywang–Jonker barrier theory, it can be inferred that the donor concentration in the grain as well as the acceptor densities at the grain boundary play a dominant role in the PTCR performance; i.e., the 'resultant' numbers of charge carriers and trap centers determine the resistivity–temperature curves significantly. Both parameters are complicated functions of the firing conditions, say, sintering temperature, soaking duration, cooling rate and ambient atmosphere, etc. [7,8]. The influence of nonstoichiometric formulations and various additives, such as different kinds and amounts of donors, the addition of 3d elements and the sintering aids, has also received attention [9–11]. Interpretations from the point of view of defect chemistry and microstructure are often offered to explain the effect of various preparing conditions [10,11].

In this study, we prepare a series of $(Ba_{0.8}Sr_{0.2})TiO_3$ PTCR samples with varying added Nd contents and discuss the donors' effect in terms of their compensating

* Corresponding author.

SSDI 0254-0584(95)01473-8

ability for the acceptor density. Excess Al_2O_3–SiO_2–TiO_2 (AST), an effective liquid phase sintering aid, is also introduced with a view to providing higher reproducibility and a lower soaking temperature. The role of AST dopants as a beneficial factor for increasing the acceptor states is emphasized. The PTCR performance, determined mainly by the properties of the semiconducting grains and insulating grain boundaries, is then interpreted as a consequence of the interaction of donor and AST additives. The resultant acceptor-state density is calculated and treated as the key parameter for the explanation of the effect of various additives.

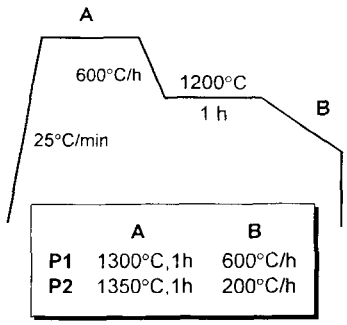

Fig. 1. The sintering profile used for the preparation of the PTCR specimens. P1 and P2 have different A and B values, as shown in the figure.

2. Experimental

PTCR specimens containing different donor concentrations varying between 0.16 and 0.28 at.% Nd were prepared with the formulation $(Ba_{0.8-x}Sr_{0.2}Nd_x)TiO_3 + y$ mol% AST. In the current study, y was selected to be 5, 7, 10 and 12. The excess AST powder serves as a liquid-phase former and was prepared by mixing Al_2O_3–SiO_2–TiO_2 in the mole ratio 4:9:3 [12,13], which was calcined at 1000 °C for 1 h. Commercially available $BaCO_3$, $SrCO_3$, Nd_2O_3 and TiO_2 were used as the starting materials. The mixture with the above-mentioned composition was mixed thoroughly in a plastic jar and mechanically ball-milled for 24 h in deionized water with plastic-coated iron ball media. The milled slurry was then dried by an IR lamp and calcined at 1100 °C for 2 h.

After being pulverized, sieved through a 140 mesh screen and pressed into a disk shape, the pellets were stacked in an Al_2O_3 crucible and then sintered in air. With the temperatures at which liquid phases occur for the BaO–TiO_2 and $BaTiO_3$–SiO_2 systems taken into consideration (1312 and 1260 °C, respectively [14,15]), it was decided to sinter the samples at 1300 or 1350 °C. Also, in light of the temperature below which the vacancy compensation dominates over the electron compensation [16], the soaking treatment was selected to be at 1200 °C for 1 h. The sintering profiles used are depicted in Fig. 1, in which P1 and P2 stand for different sintering conditions.

Resistivity–temperature (ρ–T) characteristics were measured using a Hewlett-Packard HP4140B instrument (pA meter/d.c. voltage source) from 30 to 300 °C in air using a two-probe method. An In–Ga (60:40) alloy was rubbed on both surfaces to provide ohmic contacts for testing. The resistivity is obtained from the calculated value of the resistance multiplied by a geometrical factor A/t, where A is the area of the disk and t the thickness.

The grain size is determined by the linear intercept method via scanning electron micrographs (SEMs) of polished surfaces, and the dielectric constant is measured at 10 kHz.

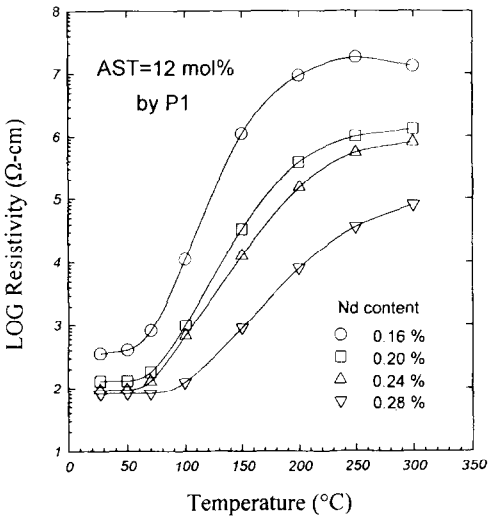

Fig. 2. PTCR characteristics as a function of the Nd concentration. The P1 profile is adopted and the AST amount is fixed at 12 mol%.

3. Results and discussion

Fig. 2 shows the resistivity–temperature (ρ–T) characteristics as a function of Nd content, while the amount of excess AST dopant is kept at 12 mol% and profile P1 is adopted. Obviously, a gradual transition in the PTCR performances can be observed; i.e., the room-temperature resistivity ρ_0 and the steepness of the rising part of the PTCR curve decrease with the Nd concentration. Also, the PTC jump, defined as $\log(\rho_{max}/\rho_{min})$, becomes smaller when more Nd is added.

The temperature coefficient of resistivity, TCR, is calculated to measure the steepness of the rising part of the ρ–T plots, given as

$$\mathrm{TCR} \equiv \frac{\ln(\rho_p/\rho_s)}{T_p - T_s}$$

where $\rho_s = 2\rho_{min}$, $\rho_p = (\rho_s \rho_{max})^{1/2}$, and T_p and T_s are the temperatures corresponding to ρ_p and ρ_s. The calculated TCR values together with ρ_0 are listed in Table 1, in which the grain size d is obtained from the typical microstructure shown in Fig. 3 (for 0.16 at.% Nd).

According to Jonker's conclusions [8] derived from the barrier theory, a higher acceptor-state density N_s will lead to a larger ρ_{max} and a lowering of the temperature at which ρ_{max} occurs, i.e., a larger TCR. A procedure to extract N_s is then developed to confirm this statement quantitatively [17,18]. The height of the potential barrier is given by

$$\phi(T) = eN_e^2/8\epsilon_0\epsilon_r n \quad (1)$$

where T is the absolute temperature in K, e the electronic charge, ϵ_0 the permittivity of free space, ϵ_r the relative permittivity of the $BaTiO_3$ material within the grain boundary layer, n the charge-carrier concentration in the bulk, and N_e the concentration of the occupied acceptor states. From the dielectric theory, as derived by Wernicke [19], the measured dielectric constant ϵ_m is substituted for ϵ_r using the following relationship:

$$\epsilon_m = \epsilon_r(d/2b) \quad (2)$$

with $b = N_e/2n$ the barrier width and d the grain size. Thus, the barrier height ϕ in Eq. (1) can be expressed in the form

$$\phi(T) = edN_e/8\epsilon_0\epsilon_m \quad (3)$$

Finally, by emphasizing the point that the PTCR effect is a grain boundary phenomenon and approximating the resistivity in terms of Eq. (3) for the ϕ expression, we have

$$\rho = \rho_0 \exp(e\phi/kT) = \rho_0 \exp[AN_e/(\epsilon_m T)] \quad (4)$$

where ρ_0 is assumed to be constant [20] and A is defined as

$$A = e^2 d/8\epsilon_0 k \quad (5)$$

which is a grain-size-dependent constant. From Eq. (4), an Arrhenius plot of ln ρ versus $(\epsilon_m T)^{-1}$ is expected to exhibit a linear relationship with a constant N_e value, and the acceptor-state density N_s can be determined from the slope provided that the constant A is known and N_s equals N_e in a certain selected temperature region, say, within T_{min} and T_{max}, as usually assumed by previous workers [21]. A typical permittivity characteristic is shown in the inset of Fig. 4 (for 0.16 at.% Nd). As seen from Fig. 4, the data points lie approximately on a straight line, which implies the validity of Eq. (4). The constant A and the slope thus obtained are listed in Table 1.

We depict the dependence of TCR and N_s on Nd content in Fig. 5, from which one can infer that the decreasing TCR caused by larger Nd content is ascribed to the resulting smaller N_s. This suggests the dual function of donor dopants: supporting the charge carrier in the grain and compensating for the acceptor at the grain boundary. This statement applies only to a certain range of donor contents, of course. Since the acceptor-state density N_s reflects the barrier height at the grain boundary, and therefore the grain boundary resistance, it is reasonable to explain the influence of Nd on the observed bulk resistivity ρ_0 in Fig. 2 via the reduction of N_s. This agrees with the results of previous works, which show that even at temperatures well below the Curie point the grain boundaries are the primary contributor to the electrical resistance [22,23].

The inset in Fig. 6 shows a schematic representation of the complex impedance plot for PTCR materials, in which the separation of the contributions from the grains and/or the grain boundaries is possible [24]. Grain boundary resistance is primarily the dominant one, and the comment near the real-axis intercept demonstrates this point. This is why the former inference of effect of Nd on ρ_0 concerns the grain boundary property and relates to the acceptor-state density N_s. A series of specimens containing various AST contents, with a view to adjusting the N_s, was then prepared using the P2 profile to examine the speculated similar dependence of ρ_0 and TCR on N_s. The results are shown in Figs. 6 and 7.

The function of AST additions as the electron traps which induce Schottky barriers accounts for the increasing ρ_0 and TCR. This rule of more AST leading to more N_s is evidently valid for 5–12 mol% AST and for all Nd contents between 0.16 and 0.28 at.%. Moreover, both ρ_0 and TCR decrease with Nd for certain AST amounts, as expected from the results in Fig. 3. It should be noted that the AST amount required to

Table 1
Room-temperature resistivity and grain size for the samples shown in Fig. 2 [a]

Nd content (at.%)	ρ_0 (Ω cm)	TCR (%/°C)	d (μm)	Constant A (10^{-6} cm^2 K)	Slope (10^7 K)	N_s (10^{13} cm^{-2})
0.16	307.45	8.9	12.3	3.23	74.29	23
0.20	115.64	6.6	11.2	2.94	35.28	12
0.24	87.28	6.1	8.5	2.23	19.4	8.7
0.28	47.86	3.9	7.5	1.97	12.4	6.3

[a] The calculated TCR and acceptor-state densities N_s are depicted in Fig. 3.

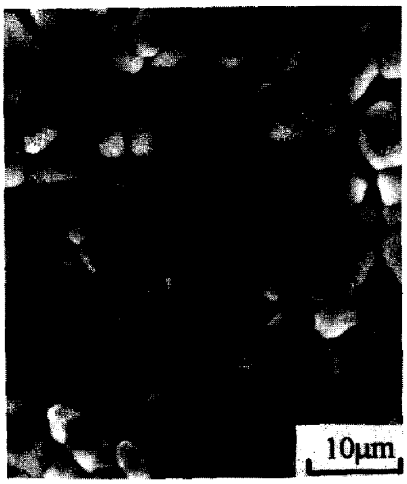

Fig. 3. Typical scanning electron micrograph of samples in the present study, for 0.16 at.% Nd.

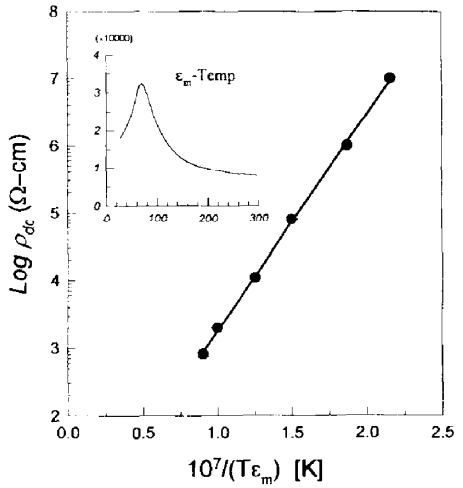

Fig. 4. Typical plots of log $\rho_{d.c.}$ vs. $(\epsilon_m T)^{-1}$ for 0.16 at.% Nd. The inset shows the dielectric constant measured at 10 kHz.

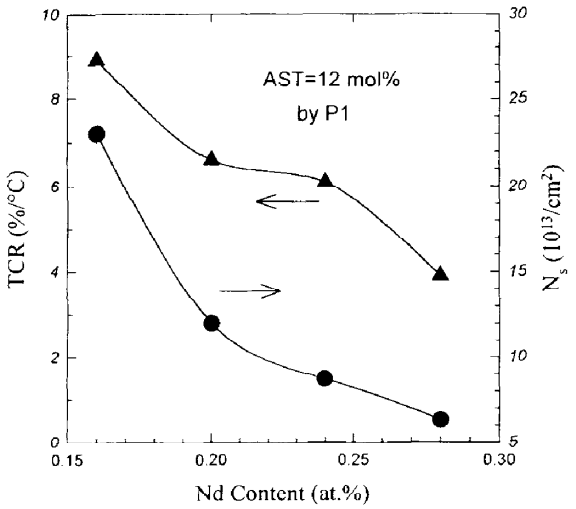

Fig. 5. TCR and calculated acceptor-state densities N_s vs. Nd content for the samples shown in Fig. 2.

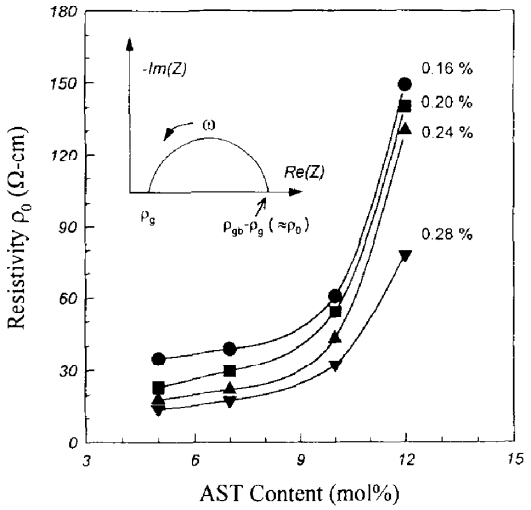

Fig. 6. Dependence of the room-temperature resistivity ρ_0 on the amount of excess AST for several Nd contents (in at.%). The P2 profile is used. The inset is the typical complex impedance plot for PTCR ceramics, in which the fact that the grain boundary resistance dominates over ρ_0 is stressed.

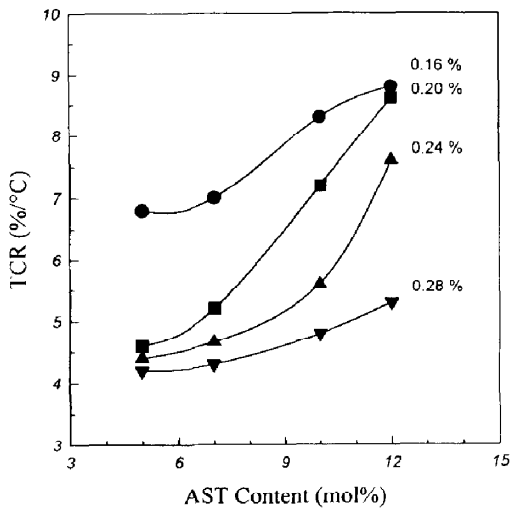

Fig. 7. Effect of AST content on the TCR. The Nd content is indicated (in at.%).

make a difference in N_s, and therefore the resulting ρ_0 and TCR, is higher than the corresponding Nd amount, i.e., the increment in Nd amount is 0.04 at.%, while there must be up to 2 mol% in the case of AST. This phenomenon probably relates to the issue of partial incorporation of Nd into the grain and the role of AST as a liquid-phase former existing at the grain boundary. It needs further research and is beyond the scope of the current study.

It is therefore concluded that, for those PTCR ceramics doped with AST sintering aids, the overall ρ–T behavior depends on the interaction of donors (Nd) and acceptors (AST). Although the TCR and PTC jumps seem to increase with decreasing Nd amount, one should note that the room-temperature resistivity

increases simultaneously. In view of the applications as a switch or current limiter for PTCR ceramics, there often exists a compromise between ρ_0 and TCR in pursuit of a 'better' ρ-T characteristic.

4. Conclusions

Investigation on the variation of the room-temperature resistivity and TCR with Nd and AST additives reveals that the electrical properties of the PTCR materials $(Ba_{0.8}Sr_{0.2})TiO_3$ are determined mainly by the grain boundary nature, which can be characterized by a useful parameter: the acceptor-state density N_s. Both ρ_0 and TCR increase with N_s. In summary, the addition of Nd donors not only makes ceramics semiconductive, but also exerts an influence on the reduction of the acceptor-state density N_s, which in turn affects the TCR value (Figs. 2 and 5). The experimental data (Figs. 6 and 7) show that AST additions act not only as the liquid-phase formers to enhance the sintering but also as useful contributors to the electron traps at the grain boundary.

Acknowledgement

This work was supported in part by the National Science Council of the Republic of China under Project No. NSC 81-0404-E009-103.

References

[1] A.L. Micheli, *Am. Ceram. Soc. Bull., 56* (1977) 783.
[2] E. Awdrich, *Philips Tech. Rev., 30* (1969) 170.
[3] O. Saubri and K. Wakino, *IEEE Trans. Component Parts, CP-10* (1963) 53.
[4] W. Heywang, *Solid-State Electron., 3* (1961) 51.
[5] W. Heywang, *J. Am. Ceram. Soc., 47* (1964) 484.
[6] G.H. Jonker, *Solid-State Electron., 7* (1964) 895.
[7] T.Y. Tien and W.G. Carlson, *J. Am. Ceram. Soc., 46* (1963) 297.
[8] G.H. Jonker, *Mater. Res. Bull., 2* (1967) 401.
[9] H. Kamioka and K. Umetani, *Jpn. Patent No. 487455* (27 Dec. 1966).
[10] T.Y. Tseng and Y.Y. Lu, *J. Mater. Sci. Lett., 7* (1988) 182.
[11] H.F. Cheng, *J. Appl. Phys., 66* (1989) 1382.
[12] Y. Matsuo, M. Fujimura, H. Sasaki, K. Nagase and S. Hayakawa, *Am. Ceram. Soc. Bull., 47* (1968) 292.
[13] W.Y. Hong and C. McCutcheon, *Ceram. Bull., 62* (1983) 231.
[14] H.M. O'Bryan and J. Thompson, *J. Am. Ceram. Soc., 57* (1974) 522.
[15] D.E. Rase and R. Roy, *J. Am. Ceram. Soc., 38* (1955) 389.
[16] J. Daniels, *Philips Res. Rep., 31* (1976) 487.
[17] C.H. Lai and T.Y. Tseng, *J. Am. Ceram. Soc., 76* (1993) 781.
[18] C.H. Lai, Y.Y. Lu and T.Y. Tseng, *J. Appl. Phys., 74* (1993) 3383.
[19] R. Wernicke, in L. Levinson (ed.), *Grain Boundary Phenomena in Electronic Ceramics*, American Ceramics Society, Columbus, OH, 1981, p. 272.
[20] D.Y. Wang and K. Umeya, *J. Am. Ceram. Soc., 73* (1990) 1574.
[21] J. Illingsworth, H.M. Al-Allak, A.W. Brinkman and J. Woods, *J. Appl. Phys., 67* (1990) 2088.
[22] H. Rehme, *Phys. Status Solidi, 26* (1968) K1.
[23] H. Ihrig and M. Kierk, *Appl. Phys. Lett., 35* (1979) 307.
[24] R.N. Basu and H.S. Maiti, *Trans. Indian Ceram. Soc., 45* (1986) 140.